Advancing Understanding of Lake-Watershed Hydrology~~Through~~ : A Fully Coupled Numerical Model Illustrated by Qinghai Lake

Lele Shu[1,2,3,†], Xiaodong Li[4,†], Yan Chang[1,2,*], Xianhong Meng[1,2,3,*], Hao Chen[1,2,3,5], Yuan Qi[1], Hongwei Wang[1], Zhaoguo Li[1,2], and Shihua Lyu[6]

[1]Key Laboratory of Land Surface Process and Climate Change in Cold and Arid Regions, Chinese Academy of Sciences, Lanzhou, Gansu 730000, China
[2]Northwest Institute of Eco-Environment and Resources, Chinese Academy of Sciences, Lanzhou, Gansu 730000, China
[3]University of Chinese Academy of Sciences, Beijing 101408, China
[4]Qinghai Institute of Meteorological Sciences, Xining, Qinghai 810001, China
[5]College of Atmospheric Sciences, Lanzhou University, Lanzhou, Gansu 730000, China
[6]Chengdu University of Information Technology, Chengdu, Sichuan 610103, China
[†]These authors contributed equally to this work.

Correspondence: * Xianhong Meng (mxh@lzb.ac.cn) and Yan Chang (changy63@lzb.ac.cn)

Abstract. Understanding the intricate hydrological interactions between lakes and their surrounding watersheds is pivotal for advancing hydrological research, optimizing water resource management, and informing climate change mitigation strategies. Yet, these complex dynamics are often insufficiently captured in existing hydrological models, such as the bi-direction surface and subsurface flow. To bridge this gap, we introduce a novel lake-watershed coupled model, an enhancement of the Simulator of Hydrological Unstructured Domains (SHUD). This high-resolution, distributed model employs unstructured triangles as its fundamental Hydrological Computing Units (HCUs), offering a physical approach to hydrological modelling. We validated our model using data from Qinghai Lake in China, spanning from 1979 to 2018. Remarkably, the model not only successfully simulated the streamflow of the Buha River, a key river within the Qinghai Lake Basin, achieving a Nash-Sutcliffe efficiency (NSE) of 0.62 and ~~0.65~~ 0.76 for daily and monthly streamflow, respectively, but also accurately reproduced the decrease-increase U-shaped curve of lake level change over the past 40 years, with an NSE of 0.71. Uniquely, our model distinguishes the contributions of various components to the lake's long-term water balance, including river runoff, surface direct runoff, lateral groundwater contribution, direct evaporation, and precipitation. This work underscores the potential of our coupled model as a powerful tool for understanding and predicting hydrological processes in lake basins, thereby contributing to more effective water resource management and climate change mitigation strategies.

Copyright statement. TEXT

1 Introduction

Lakes, as crucial components of the global hydrosphere, occupy only a small fraction of the earth's surface though, they play an indispensable role in the water cycle (Grant et al., 2021; Woolway et al., 2021; Pi et al., 2022). They are particularly susceptible to the impacts of climate change and anthropogenic activities, underscoring their significance in the global ecological balance. These water bodies serve as sensitive indicators of environmental changes, and their health and sustainability are of paramount importance (Li et al., 2022; Jones et al., 2022; Woolway, 2023). The study of lake hydrology, therefore, is not only a scientific endeavor but also a necessity for effective environmental management and policy-making (Crowe and Schwartz, 1981; Carter, 1986; Qi et al., 2020).

The development and application of coupled lake-watershed models have emerged as a powerful approach to understanding the complex interactions between lakes and their surrounding landscapes. These models integrate various hydrological processes, including surface runoff, groundwater flow, and lake-water interactions, thereby providing a holistic understanding of the basin system. The use of such models has proven instrumental in studying regional water resources, nutrient loads in lakes and groundwater, hydrologic connectivity of lake systems, and the impact on local economies (Dong et al., 2019; Cobourn et al., 2018; Ladwig et al., 2021).

However, the development and application of these models are not without challenges. One of the key issues is the accurate representation of subsurface groundwater flow, which often has a more significant impact on lake water and chemical budgets than surface water inflow. Furthermore, the relative importance of surface water vs. groundwater, and watershed vs. in-lake processes needs to be accurately captured for effective lake understanding and management (Johnston and Shmagin, 2006).

Over the past few decades, the development of lake-watershed models has significantly advanced, driven by a growing recognition of their importance in understanding and managing aquatic ecosystems. These models have evolved from simple, lumped or semi-distributed models to more complex, spatially distributed models that can simulate a wide range of hydrological processes (Lewis et al., 1984; Kratz et al., 1997). Various researchers have further expanded upon this foundation. A noteworthy example is the WATLAC model, devised by Zhang and Werner (2009), which can emulate surface and subsurface fluxes into a lake, and fathom the interaction between a watershed and its lake (Ye et al., 2011). Similarly, the Soil and Water Assessment Tool and the Snowmelt Runoff Model have been used to simulate the water equilibrium within a lake's watershed (Zhang et al., 2014; Dargahi and Setegn, 2011). In a more recent work, one-way coupling was accomplished using the MGH-IPH hydrological model and the IPH-ECO hydrodynamic model, with application to Lake Mirim, in South America (Possa et al., 2022; Munar et al., 2018). Wu et al. (2017) integrated the hydrological model HIMS with a hydrodynamic model to examine water exchange in the Hongfeng Reservoirs. Xu et al. (2007) coupled the HSPF and CE-QUAL-W2 model to simulate the hydrodynamics and water quality in Lake Manassas and the Occoquan Reservoir in Virginia, USA. Chauvelon et al. (2003) combined the HIC and RMA2 model to replicate the Vaccares lagoon level and salinity, while Inoue et al. (2008) implemented a coupled hydrology-hydrodynamic model to simulate the hydrology and hydrodynamics in the Barataria Basin, USA. Dargahi and Setegn (2011) constructed the SWAT+GEMSS model to simulate Lake Tana, Ethiopia. These models have been instrumental in shedding light on the water cycle and runoff mechanisms in various lake basins, thereby illuminating

the environmental issues plaguing these regions (Cui and Li, 2015a). Despite these advancements, further research is needed to improve the accuracy and reliability of these models, particularly in the challenges of lake-watershed bi-directional water exchange.

The conventional approach in these studies has been to leverage hydrological models to calculate the runoff to the lake, with the results then serving as boundary conditions in the hydrodynamic model. Such models typically consider the lake as an isolated water body, separate from the basin's water cycle, thus assuming that lake fluctuations do not influence watershed groundwater or river discharge. In essence, most of these models operate on a one-way coupling scheme. However, a recent advancement by Ladwig et al. (2021) deviates from two-way coupling norm. They developed the PIHM-Lake model for bi-directional hydrological interactions between lake and watershed, and coupled it with a one-dimensional hydrodynamic-ecological model (GLM-AED2), which simulates the thermal and water quality dynamics of Lake Mendota in the USA. Uniquely, this model is capable of simulating both river runoff and fluxes in the lake's surrounding watershed.

Though a fully coupled lake-watershed hydrological model may not offer the highest resolution as typical of hydrodynamic models, it should accurately represent the bi-directional water exchange—encompassing surface, subsurface, and rivers—between the lake and its watershed. The combination of lake and hydrological models can simulate the lake's hydrology and surrounding landscape over time, thereby informing decisions geared towards the preservation of the lake's water quality and ecosystem health. This holistic understanding of bi-directional hydrological processes provides critical guidance for management decisions aimed at maintaining both the water quality and ecological health of the lake.

~~The goal of this study is~~ This study aims to develop and validate a fully coupled lake-watershed hydrological model, ~~with the newly devised numerical model tested in Qinghai Lake, China. The~~ using Qinghai Lake in China as the test site. As the largest lake in China, Qinghai Lake's unique hydrological and environmental features make it an ideal candidate for this purpose. Its endorheic nature simplifies the lake-watershed connections, aiding in the model's testing. The extensive existing research data on Qinghai Lake's hydrology, ecology, and climate is instrumental for the model's calibration and validation. Additionally, the lake's characteristics as a high-altitude, cold, and arid region make it a representative model for similar environments, enhancing the model's interdisciplinary research potential and broadening its applicability.

The methodologies employed in the modeling process are thoroughly expounded upon in Section 2, while Section 3 showcases the simulation results for Qinghai Lake. Section 4 offers a discussion on the limitations of the model and potential areas for future enhancement.

2   Methods

2.1   Research Area

Qinghai Lake, the largest saline lake in China, is nestled within the Qinghai-Tibet Plateau in northwest China. Covering an expansive area of approximately 4,489 ~~km^2~~ km^2 and plunging to a maximum depth of 32 ~~m~~ m, this lake has emerged as a significant hydrological and environmental research hub. It has been the subject of extensive multidisciplinary research

spanning hydrology, climate science, meteorology, limnology, ecology, and biogeochemistry (Zhang et al., 2014; Qi et al., 2020; Su et al., 2020; Wang et al., 2022).

The hydrological equilibrium of Qinghai Lake is primarily sustained by several rivers and streams, with no outlets. The
85 Buha River is the most substantial contributors, responsible for ~~49~~49% of the total inflow into Qinghai Lake ~~, approximately~~ (Wang et al., 2022). The lake's water balance is intricately woven with precipitation, evaporation, and river discharge. As such, shifts in climate and land use patterns can profoundly influence this balance. The lake's climate, typified by an average annual temperature of approximately -2.5 °C and an average annual precipitation of 415 ~~mm~~ mm (based on CMFD reanalysis data, 1919-2018), is largely dictated by the Asian monsoon system, with the majority of rainfall occurring during the summer
90 months. Climate alterations, such as temperature escalations and precipitation pattern changes, can significantly affect the lake's water balance, ecology, and biogeochemistry ~~Su et al. (2019, 2020)~~(Su et al., 2019, 2020).

Qinghai Lake, a unique ecosystem with a high degree of endemism, provides a haven for a diverse array of endemic fish and bird species. Changes in the lake's water chemistry and hydrology can have substantial impacts on its ecology. Consequently, Qinghai Lake serves as a pivotal research site for exploring the complex interconnections between hydrology, climate,
95 meteorology, limnology, ecology, and biogeochemistry in high-altitude, cold, and arid regions.
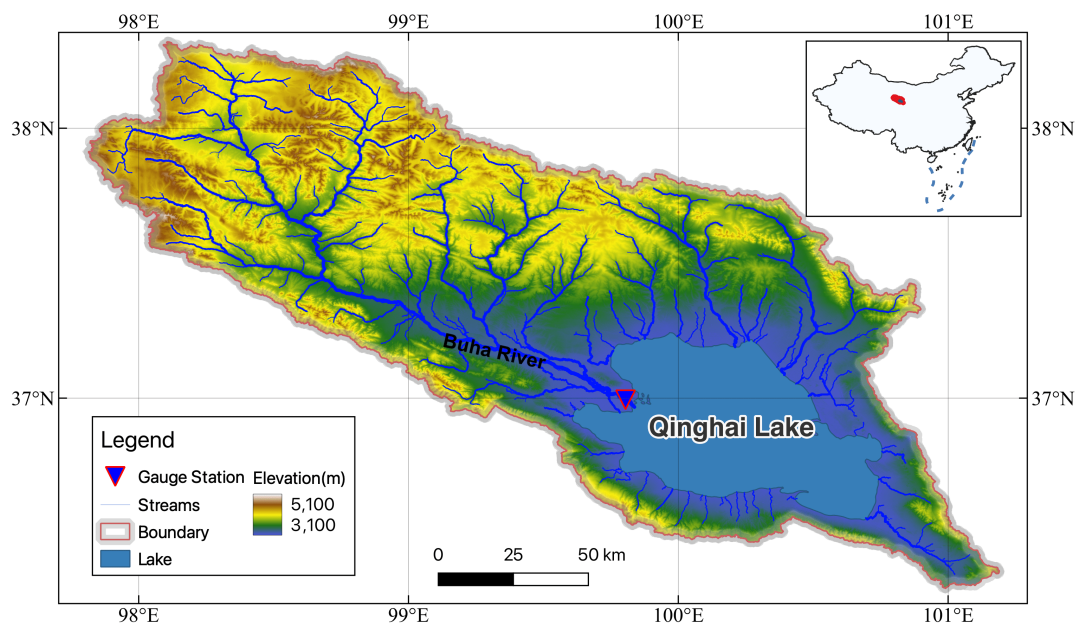
Figure 1. Research Area map with elevation, river network, and stream gauge stations.

2.2   SHUD Model

The Simulator for Hydrologic Unstructured Domains (SHUD) is a comprehensive, multi-scale ~~hydrological model~~ , integrated surface-subsurface numerical hydrological model (ISSNHM) that employs the Finite Volume Method ~~.~~ and unstructured triangular mesh. The merits of ISSNHMs lie in their temporal-spatial continuum, contrasting with other semi-distributed models like SWAT, TOPMODEL, VIC etc. (Freeze and Harlan, 1969; Hrachowitz and Clark, 2017). This model, an evolu-
tion of the computational strategy developed by Qu and Duffy (2007) for the Penn State Integrated Hydrologic Model (PIHM), provides a more accurate depiction of a watershed's physical attributes, such as topography and land use patterns (Shu et al., 2020). The SHUD model's capacity to simulate both surface and subsurface hydrological processes renders it a valuable tool for examining interactions between groundwater and surface water. Additionally, its adaptive time-step (seconds to minutes) feature enhances computational efficiency by adjusting the time-step in response to the complexity of the simulated processes, thereby ensuring precise representation of both rapid and slow hydrological processes. The details and performance of the SHUD model can be found in Shu et al. (2020).
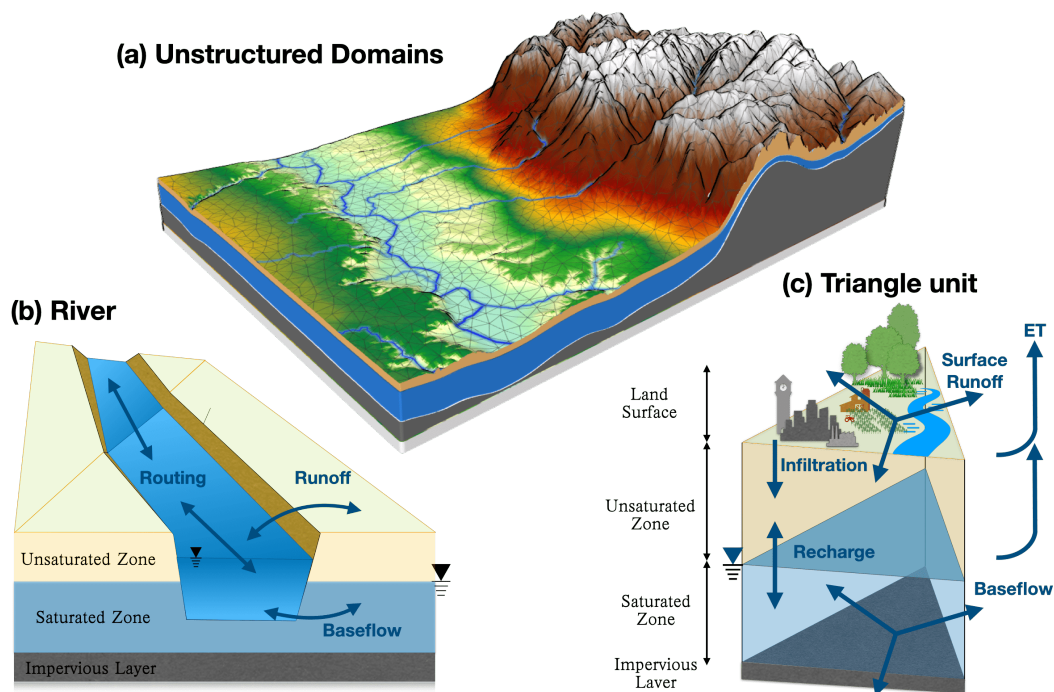
Figure 2. The structure of SHUD model; (a) the triangular mesh in watershed scale, (b) the flux exchange between river and hill-slope elements, (c) the three-layer triangular element.

In SHUD V 1.0, there are two types of Hydrological Computing Units (HCUs): triangular slope elements and trapezoid segments for river reaches. Each triangular HCU is further divided into three layers: land surface, unsaturated zone, and

saturated zone. Therefore, the total number of HCUs in a watershed model is $N = 3 \times N_{ele} + N_{riv}$, where N_{ele} is the number of triangular elements, and N_{riv} is the number of river reaches. The terminology *element* and *cell* are used interchangeably in our model, both referring to the unstructured triangle.

The primary task of the SHUD model as a numerical hydrological model is to calculate the fluxes among the HCUs. The land surface layer computes snow accumulation/melting, interception, infiltration, and lateral fluxes to triple neighbor elements. The unsaturated zone only calculates vertical infiltration/exfiltration and recharges to the saturated zone. The saturated zone calculates the lateral groundwater flow (or baseflow) among the triangular elements. Both the unsaturated and saturated zone response to the potential ~~evapotrianspiration~~evapotranspiration, based on the water content and groundwater level.

To model a lake within a basin context, a model must define the two-dimensional area of the lake domain and the respective boundary conditions, including water levels, inflows, and outflows. Information on the physical characteristics of the lake, such as its volume, surface area, and depth, must also be provided. Once the lake domain has been established, hydrological processes within and around the lake can be simulated, including precipitation, evaporation, runoff, and groundwater flow. Furthermore, the model simulates the movement of nutrients, sediment, and other substances within the lake. To execute the SHUD model accurately, input data on topography, climate, land use, and soil properties must be provided. This data is crucial for simulating the hydrological processes in the lake and the surrounding landscape. The coupled model output provides a deeper understanding of the lake's hydrology, and different management strategies can be assessed to determine their impact on the lake's ecosystem health and water quality.

2.3 Lake Coupling

In the context of the SHUD model, lake coupling involves integrating the lake model with the hydrological model to simulate the lake's water balance and its influence on surrounding hydrological processes. This enhanced model, which couples a lake module with SHUD, treats the lake as a distinct entity within the model domain, complete with its own set of governing equations and boundary conditions. The lake model simulates the hydrological processes occurring within the lake, such as evaporation, inflows, outflows, and water storage. Concurrently, the hydrological model simulates the processes unfolding in the surrounding landscape, including precipitation, interception, evapotranspiration, surface runoff, groundwater flow, and river routing. The model also accounts for the inflows and outflows to and from the lake.

The water balance of the lake is generally defined by the following equation:

$$\frac{\Delta S}{\Delta t} = A_b(P - E) + Q_s + Q_g + R_i - R_o \tag{1}$$

where ΔS represents the change in storage within the time interval $[L^3]$; Δt is the time interval $[T]$; A_b is the area of lake bucket $[L^2]$; P is the precipitation rate $[LT^{-1}]$; E is the actual evaporation on lake surface $[LT^{-1}]$; Q_s is the surface direct runoff from the surrounding land to the lake $[L^3T^{-1}]$; Q_g is the total groundwater flux into the lake $[L^3T^{-1}]$; R_i is the total water fluxes into the lake $[L^3T^{-1}]$; and R_o is the total fluxes from the lake into the downstream rivers $[L^3T^{-1}]$, which is zero for a closed lake. Therefore, the essential task for lake hydrological modeling is to calculate the flux items between the surrounding land and the lake.
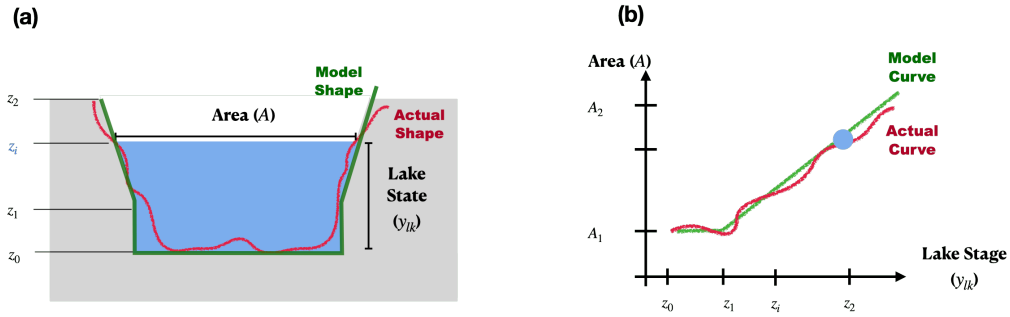
Figure 3. Representation of lake geometry in the coupled model. The lake is portrayed as a bucket (a), its form determined by a bathymetry curve (b) that associates lake stage (y_{lk}) or elevation (z) with surface area.

2.3.1 Hydrological Computing Unit

Within the computational domain of the coupled SHUD model, a lake is conceptualized as a "bucket" (Fig. 3). This "bucket" is geometrically defined by the lake's bathymetric curve, which establishes a relationship between the lake stage and its surface area (Fig. 3 (b)). The bathymetric curve used in the model might be a simplified representation of the actual curve. For each specified lake stage, a corresponding top surface area is determined. Utilizing this curve, we can compute the volume of lake water ($V(y)$) by accounting for the fluxes into and out of the lake over a designated time interval (Eq. 2). Concurrently, the fluctuation in the lake stage (y or y_{lk}) can be gauged by simulated changes in the lake's volume ($V(y)$) . However, alterations in the lake's surface area ($A(y)$) do not impact the boundary delineation between the lake and the neighboring land within the model. The dynamic expansion and contraction of lakes are not considered within the internal and adjacent elements of the lake domain.

$$V(y) = \int\limits_{0}^{y} A(y) \cdot dy \tag{2}$$

In order to enable lake coupling, a novel Hydrological Computing Unit (HCU) that represents the lake has been integrated into the numerical solver. The lake HCU encapsulates the lake itself, with the water fluxes within the HCU representing the cumulative sum of all the triangular elements contained within the lake.

Within the coupled model, the triangular units are classified into land, bank, and lake elements (Fig. 4(a)), the element distinguished by a flag that indicates its type. The computational algorithms diverge significantly among these element types. Land elements conform to the standard triangular elements found in the SHUD model (Shu et al., 2020). Bank elements, which exist in a transitory state between the land and lake, are processed using a specialized method. The surface and subsurface fluxes over the lake-facing edges of a bank element are computed based on the hydraulic disparity between the bank and lake elements.

Conversely, the vertical fluxes, including precipitation and evaporation, are handled within the lake element, while the lateral fluxes (comprising surface and subsurface fluxes between bank and lake elements) are directly addressed within the lake HCU.
165 Notably, although a lake HCU consists of multiple triangular units, the lake's hydrology is considered holistically. This implies that the water stage of each triangular lake element is congruent. Precipitation and evaporation occurring on the lake surface correspond to the summation of the vertical fluxes across the lake units.
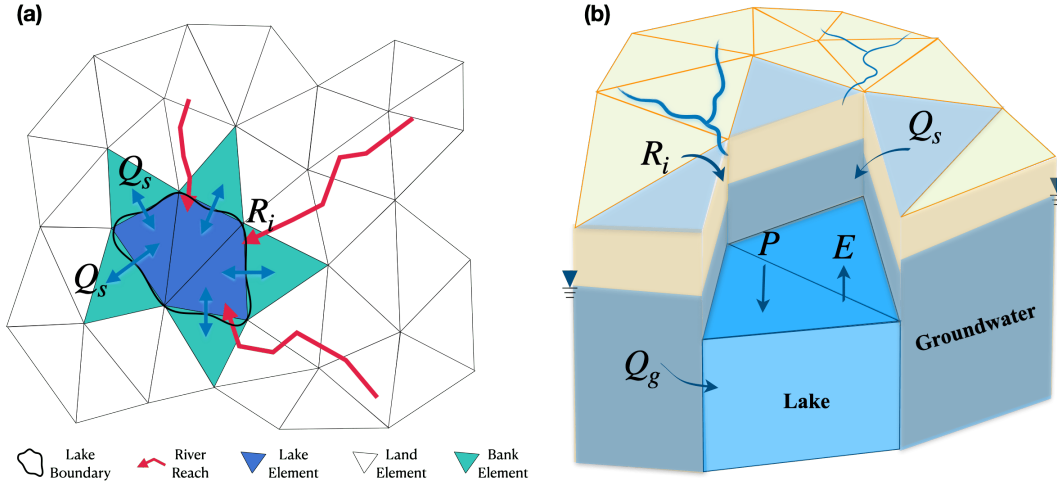
Figure 4. Depiction of elements and fluxes within the coupled domains. (a) Illustration of the three types of triangular elements: land, bank, and lake elements. (b) A 3D perspective of these elements along with the fluxes interacting among them.

2.3.2 Fluxes Calculation

The correct synchronization of the lake and hydrological models requires defining the water exchange between the lake and
170 the surrounding landscape, which includes factors like surface runoff and groundwater flow (Fig. 4 (b)). Calculations for these exchanges start with the lake's water balance (Eq. 1). These fluxes can then be split into the sum of the fluxes on each lake element (Eq. 4).

$$\frac{\Delta S}{\Delta t} = A_b(P-E) + Q_s + Q_g + R_i - R_o \tag{3}$$

$$= \sum_{j=1}^{N_l} P^j A^j + \sum_{j=1}^{N_l} E^j A^j + \sum_{j=1}^{N_b} Q_s^j + \sum_{j=1}^{N_b} Q_g^j + \sum_{j=1}^{N_r} R_i^j + 0 \tag{4}$$

175 In this formula, N_l, N_b, and N_r represent the number of lake elements, bank elements, and river outlets into a lake, respectively. P^j is the precipitation falling into a lake element with an area of A^j. Within the SHUD model, the potential evapotranspiration (PET) is calculated using the Penman-Monteith equation, and the actual evapotranspiration (AET) on each lake element is equivalent to the PET on it. The sum of the AET of all lake elements becomes the total AET of the lake.

The total overland runoff to a lake is comprised of the sum of overland fluxes between the bank elements and the lake. In a similar vein, the aggregate groundwater flow from the land to the lake is calculated as the sum of the groundwater fluxes between the bank and lake elements. This calculation is contingent on their respective hydraulic heads, terrains and hydraulic characteristics.

$$Q_s^e = C_{wr} L_e y_{sf}^{\frac{3}{2}} \sqrt{2g} \tag{5}$$

$$Q_g^e = \overline{K} \cdot \frac{(y_{gw} + z_b) - (y_{lk} + z_b^l)}{d_l} \cdot \left[\frac{L_e}{2} (y_{gw} + y_{lk}) \right] \tag{6}$$

$$Q_r = \frac{A_{cs}}{n} \left(\frac{A_{cs}}{p_w} \right)^{\frac{2}{3}} s_r^{\frac{1}{2}} \tag{7}$$

In these equations, Q_s^e and Q_g^e represent the overland runoff and groundwater flow in e direction ($e = C(1,2,3)$) of a triangular element, expressed in units of volume per time $[L^3 T^{-1}]$; Q_r stands for the discharge from the river to the lake. The terms y_{sf}, y_{gw}, and y_{lk} denote the water head of surface ponding from the land surface, the groundwater head from bedrock, and the lake hydraulic head or lake stage from the lake-bed, respectively, all expressed in length units $[L]$. C_{wr} is the discharge constant for weir flow $[-]$, and n represents Manning's roughness $[TL^{-1/3}]$. L_e is the length of a triangle's edge in e direction $[L]$; $\overline{K}$ is the average hydraulic conductivity of a bank element and its adjacent lake element $[LT^{-1}]$; z_b and z_b^l are the elevations of the bank element bedrock and the lake-bed $[L]$, respectively; d_l is the distance between the centroids of a bank element and its neighboring lake element $[L]$; A_{cs} is the cross-sectional area of river flow; p_w is the wetting-perimeter in a river channel $[L^2]$; and s_r is the hydraulic gradient $[LL^{-1}]$.

2.4 Numerical solver

In SHUD, the initial value problem for these ordinary differential equations (ODEs) is formulated as follows:

$$\frac{d\boldsymbol{Y}}{dt} = f(t, \boldsymbol{Y})$$

$$\boldsymbol{Y}(t_0) = \boldsymbol{Y_0}.$$

Here, the discrete state vector is denoted by $\boldsymbol{Y}$:

$$\boldsymbol{Y} = \begin{pmatrix} \boldsymbol{Y_{sf}} \\ \boldsymbol{Y_{us}} \\ \boldsymbol{Y_{gw}} \\ \boldsymbol{Y_{riv}} \end{pmatrix}.$$

$\boldsymbol{Y_0}$ represents the initial conditions, and $f(t, \boldsymbol{Y})$ denotes the equations governing the hydrologic flow.

In the coupled model, the $\boldsymbol{Y}$ value is updated with the added $\boldsymbol{Y_{lk}}$, so the new $\boldsymbol{Y}$ is:

$$\boldsymbol{Y} = \begin{pmatrix} \boldsymbol{Y_{sf}} \\ \boldsymbol{Y_{us}} \\ \boldsymbol{Y_{gw}} \\ \boldsymbol{Y_{riv}} \\ \boldsymbol{Y_{lk}} \end{pmatrix}.$$

The $\boldsymbol{Y}_{lk}$ represents the lake stage of all lakes in the model domains. For instance, if there are three lakes in the domains, then $\boldsymbol{Y_{lk}}$ is:

$$\boldsymbol{Y_{lk}} = \begin{bmatrix} y_{lk}^1 \\ y_{lk}^2 \\ y_{lk}^3 \end{bmatrix}.$$

The change in the lake stage, $d\boldsymbol{Y_{lk}}$, is:

$$d\boldsymbol{Y_{lk}} = \begin{bmatrix} dy_{lk}^1 \\ dy_{lk}^2 \\ dy_{lk}^3 \end{bmatrix}.$$

200   In this equation, $dy_{lk} = \frac{\Delta S}{A(y)}$, where $A(y)$ is the lake top area when lake stage equates y, which is based on the defined lake bathymetry curve. The length of both vectors $\boldsymbol{Y}$ and $d\boldsymbol{Y}$ equals N, where $N = 3 \times N_{\text{ele}} + N_{\text{riv}} + N_{\text{lk}}$. The N is the total length of HCUs in the coupled model.

In the coupled model, lake elements serve as agents for flux calculation, with fluxes computed based on the properties of these elements. However, the mass balance of the lake element is omitted, and the fluxes are instead incorporated into the lake's

205   water balance. As a result, the y_{sf}, y_{us}, and y_{gw} values of the lake elements remain constant in the vectors $\boldsymbol{Y_{sf}}$, $\boldsymbol{Y_{us}}$, and $\boldsymbol{Y_{gw}}$. These unvarying values, albeit constant, do not impede the calculations or the efficiency of the numerical solver and remain at zero in the $d\boldsymbol{Y}$ vector.

Upon completion of the new vectors $\boldsymbol{Y}$ and $d\boldsymbol{Y}$, the task of handling iterations and outputting the results of each step is transferred to the CVODE numerical solver (Hansen, 2016), a tool developed by the Lawrence Livermore National Laboratory

210   (LLNL) for initial condition problems. The initial condition of the lake, indicating the lake stage at the outset of the simulation, is stored in conjunction with the initial conditions of other HCUs in the *.cf.ic* files.

2.5   Data

The SHUD modelling framework employs three distinct categories of data: meteorological forcing data, terrestrial data, and observational data. The latter serves to facilitate model calibration and the configuration of initial conditions.

215   Meteorological forcing data were sourced from the China Meteorological Forcing Dataset (CMFD) (He et al., 2020) due to the limited availability of in-situ meteorological stations within the study area. The CMFD incorporates variables such as precipitation, air temperature, specific humidity, short-wave radiation, wind speed, and air pressure, providing sufficient variables to drive the SHUD model. Despite the CMFD's extensive coverage of China and high-quality reanalysis, it has an

inclination to underestimate rainfall intensities, which can potentially lead to an underestimation of peak stream discharge. The

220 dataset is characterised by a 6-hour time interval and a 0.1-degree horizontal resolution, resulting in a total of 386 CMFD grids within the simulation domains (Fig. 5).

Terrestrial data was gathered from the Global Hydrological Data Cloud (https://shuddata.com, accessed June 10, 2023). The Digital Elevation Model (DEM) was derived from the ASTER Global DEM (NASA et al., 2018), providing a resolution of 3-arc-seconds (approximately 30 meters). Soil classification and texture data were extracted from the Harmonized World Soil

225 Database v1.2 (Nachtergaele et al., 2008), offering a ~~1-*km*~~ 1-km resolution. The 0.5-~~*km*~~ km USGS MODIS land cover dataset (Broxton et al., 2014) was the source of land cover data, integral to the model deployment process.

Observational streamflow data was acquired from the Buha gauge station ~~, located at 99°44′13″E, 37°02′13″N~~ (see the location in Figure 1). This dataset, encompassing daily streamflow measurements from 1980 to 2017, was obtained from a local gauge station and is currently not publicly accessible. Hydrological data specific to Qinghai Lake was sourced from

230 the Qinghai Lake hydrology-meteorological dataset (Zhang, 2021). The lake, with an average area of 4360 ~~km^2~~ km^2 and an average lake level of 3195 ~~*m*~~ m, recorded its lowest level of 3192.86 ~~*m*~~ m in 2004. This dataset (Zhang, 2021) provides invaluable insights into the hydrological dynamics of Qinghai Lake, contributing to a nuanced understanding of the lake's hydrological and environmental significance.

2.6 Model Deployment

235 The SHUD model was deployed using the rSHUD package and the AutoSHUD script, with the corresponding R script and terrestrial data accessible as per ~~Shu (2023b)~~ Shu et al. (2023); Shu (2023b).

~~Figure 5 elucidates the~~ The domain decomposition results for the Qinghai Lake Basin (QLB) ~~. The model domain comprises~~ consists of 4773 triangular elements, ~~with~~ of which 688 ~~earmarked~~ are designated as lake elements and 785 as bank elements ~~. The~~ (Figure 5). The domains encompass a total lake area of 4404 km^2, with the surrounding watershed area accounting for

240 25210 km^2. While Figure 5 might seem similar to Figure 1 at first glance, it specifically represents the unstructured triangular mesh model domains constructed by the rSHUD tool (Shu et al., 2023), highlighting the computational framework applied in our study. The average area of the triangular elements within the model domain is 6.2 ~~km^2~~ km^2. The river network within the domain, spanning a total length of 4122 ~~*km*~~ km, features an average river reach length of approximately 2.5 ~~*km*~~ km. The model incorporates 1633 river reaches and 45 river outlets, all ~~of which feed~~ feeding into the lake.

2.7 Calibration

The model's initial condition is established using the state after a preliminary 40-year simulation (from 1979 to 2018). Specifically, the state at the end of this simulation period (December 21, 2018) is employed as the initial condition for both calibration and long-term simulation. The initial lake stage is set 25 ~~*m*~~ m above the lowest point of the lake bed, corresponding to a lake level of 3183 m.

250 Model calibration was performed using the Covariance Matrix Adaptation - Evolution Strategy (CMA-ES) (Hansen, 2016). This evolutionary algorithm produces 96 offspring in each generation, maintaining the best-performing offspring as the seed
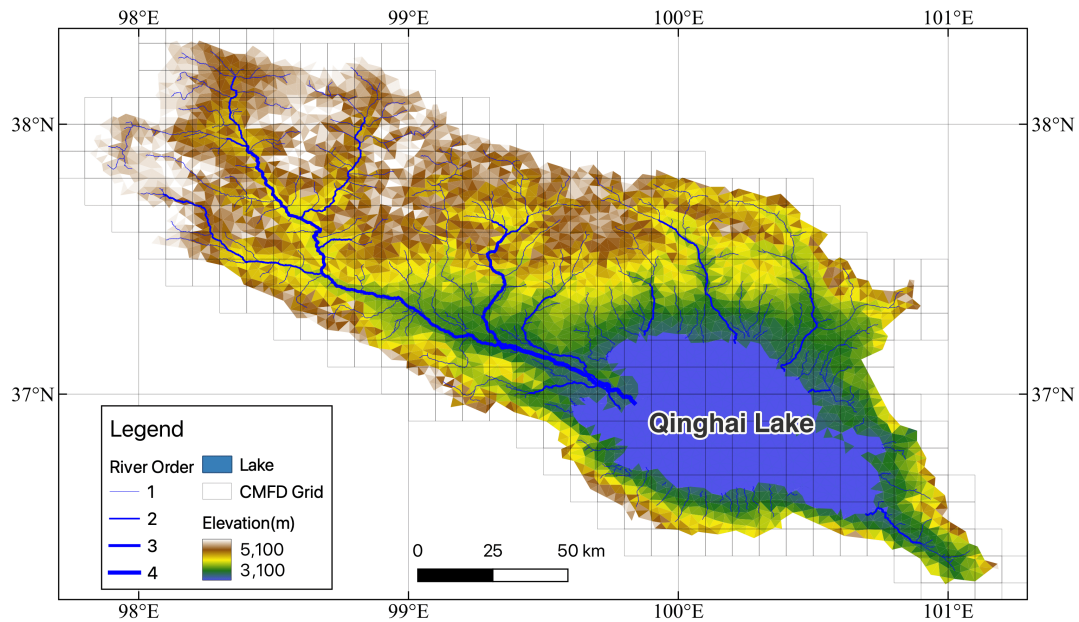
Figure 5. The rSHUD-constructed unstructured domains in the Qinghai Lake Basin, comprising 4773 triangular elements of which 688 are designated as lake elements and 785 as bank elements.

for the subsequent generation with additional perturbations. These perturbations are derived from the covariance matrix of the previous generation. The calibration period extends from 2004 to 2008, with two validation periods: 1980-1999 and 2009-2017. The first validation period is 20 years prior to the calibration period, while the second follows 9 years after. The calibration

255 begins with a CMA-ES calibration for the period 2002-2008, using 2002-2003 as the spin-up period. After 14 generations of CMA-ES iterations, the calibration tool identifies an optimal parameter set. This parameter set is then utilized for the 40-year simulation, after which the model's performance is analyzed.

~~Figures 6 and 7 show the~~ The model's ~~performance in simulating~~ ability to simulate daily and monthly discharges in the Buha River ~~,~~ is demonstrated in Figures 6 and 7 respectively. During the calibration period, three goodness-of-fit (GOF)

260 indicators - Nash-Sutcliffe efficiency (NSE, Nash and Sutcliffe (1970)), Kling-Gupta Efficiency (KGE, Gupta et al. (2009)), and Determination Coefficient (R^2) - yield values of 0.62, 0.58, and 0.65, respectively (Fig. 6). The GOF of daily streamflow in the validation period is lower than that in the calibration period (as expected), with NSE = 0.41/0.46, KGE = 0.44/0.52, and R^2 = 0.46/0.47. As anticipated, the monthly GOFs are higher than the daily GOFs, with NSE = 0.76, KGE = 0.64, and R^2 = 0.82 for the calibration period, and NSE = 0.56/0.56, KGE = 0.54/0.59, and R^2 = 0.63/0.57 for the validation periods.
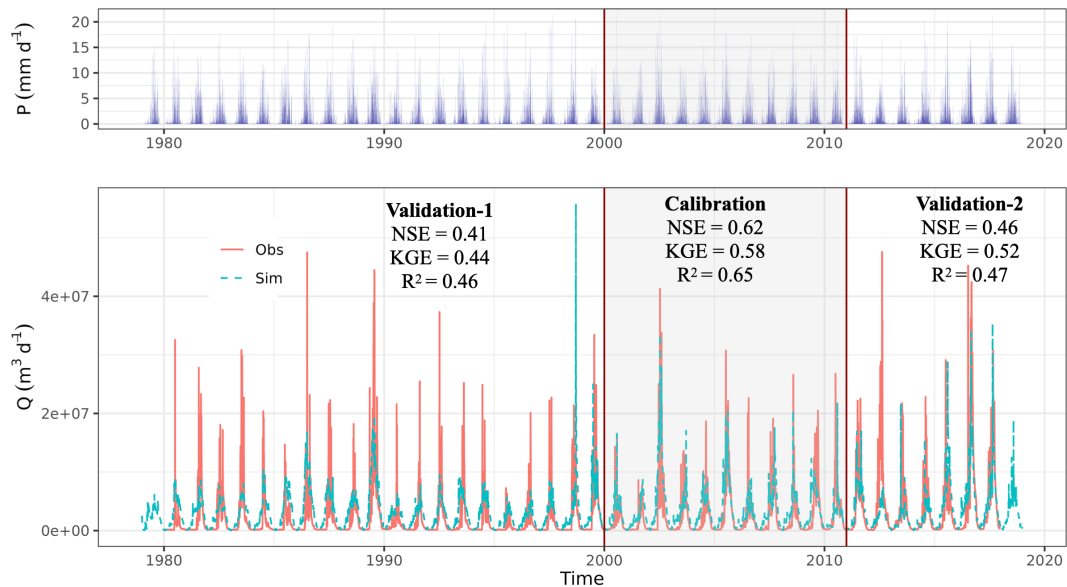
Figure 6. The hydrograph of daily discharge in Buha River during calibration and validation periods.

3 Results

In this study, we primarily aim to simulate lake dynamics by employing the developed lake-watershed coupled model. We have previously presented the simulation results of stream flow in the calibration section, and hence, this section centers on lake-specific outcomes, namely the alterations in lake level and the components of the lake's water balance.

3.1 Lake level

Figure 8 delineates the simulated temporal variations in lake level. Our observational dataset extends from 1960 to 2020, however, the simulation period is confined to 1979-2018, conditioned by the availability of CMFD data. We define the mean lake level in 2000 as the benchmark level, and all changes in lake level are computed relative to this datum point. In multi-decades simulations, the change in lake water mass is more valuable and reliable than elevation above sea level. According to the lake settings, the lake is depicted as a bucket determined by lake stage and top area. Without detailed bathymetry (function of lake stage and top area), we can only roughly describe the lake shape (Figure 3). The rough estimation of lake bathymetry introduces an error in simulating lake surface elevation. Moreover, the DEM and lake level measurements, sometimes based on different datum, exhibit discrepancies. The key target in lake hydrology is not the water level elevation, but the change in lake water
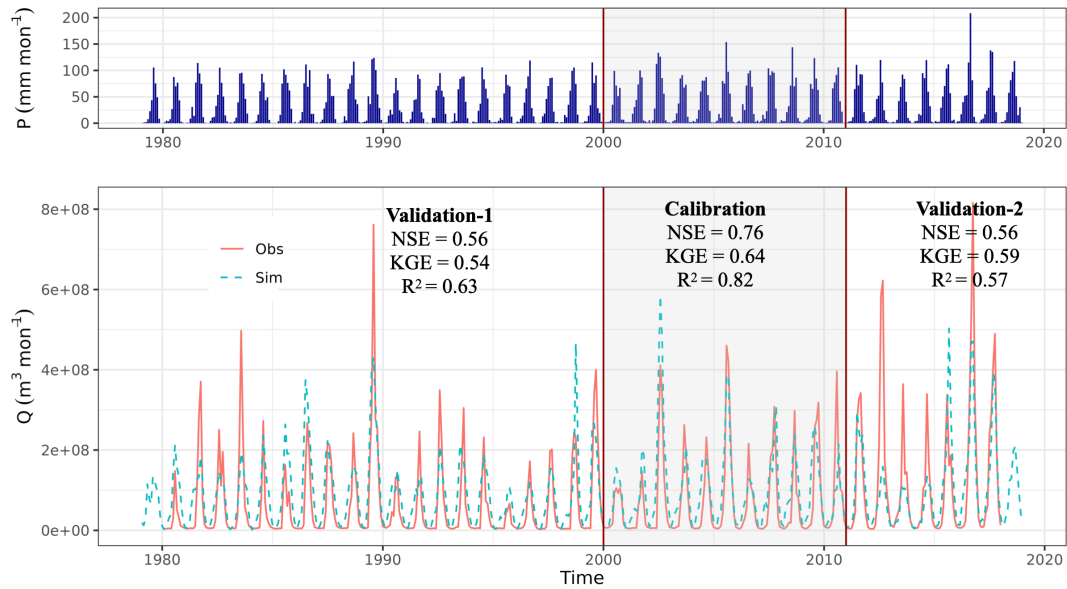
Figure 7. The hydrograph of monthly discharge in Buha River during calibration and validation periods.

volume, i.e., the lake water balance. In the results, the changes in lake water volume are more reliable than the absolute values of lake water level in the coupled model, hence Figure 8 compares the fluctuations in water level.

280 In general, the simulated lake level variations exhibit a high degree of alignment with the observed changes, tracing a decrease-increase U-shaped trajectory. Nonetheless, a minor underestimation of the lake level is observed at the begining of the simulation period (Fig. 8 (a)). The line-fit plot (Fig. 8 (b)) offers further insight into the model's proficiency in replicating lake level alterations, with GOF values of NSE = 0.71, KGE = 0.63, and R^2 = 0.77.

3.2 Water balance of the lake

285 The perspective of water balance is indispensable for deciphering the hydrological attributes of a lake within a basin. As outlined in Eq. 1, the water balance is partitioned into six constituents: fluctuations in lake storage (ΔS), precipitation (P), evaporation (E), ~~precipitation, evaporation,~~ and contributions from rivers (R_i), surface runoff (Q_s), and groundwater flow (Q_g). Throughout the simulation period (1979-2018), the lake level escalated by ~~1540 mm~~1696 mm, a balanced outcome derived from the interplay of the other five components. The mean annual precipitation ~~and evaporation are approximately 350~~

290 ~~mm and 904 mm~~(P) and evaporation (E) are approximately 386 mm and 996 mm, respectively, with the latter aligning with values reported in the literature (Dong et al., 2019; Su et al., 2019). The annual precipitation over the lake ~~form~~ from the CMFD dataset is less than the basin average precipitation. Contributions from rivers (R_i) amount to about ~~533 mm per annum~~587 mm
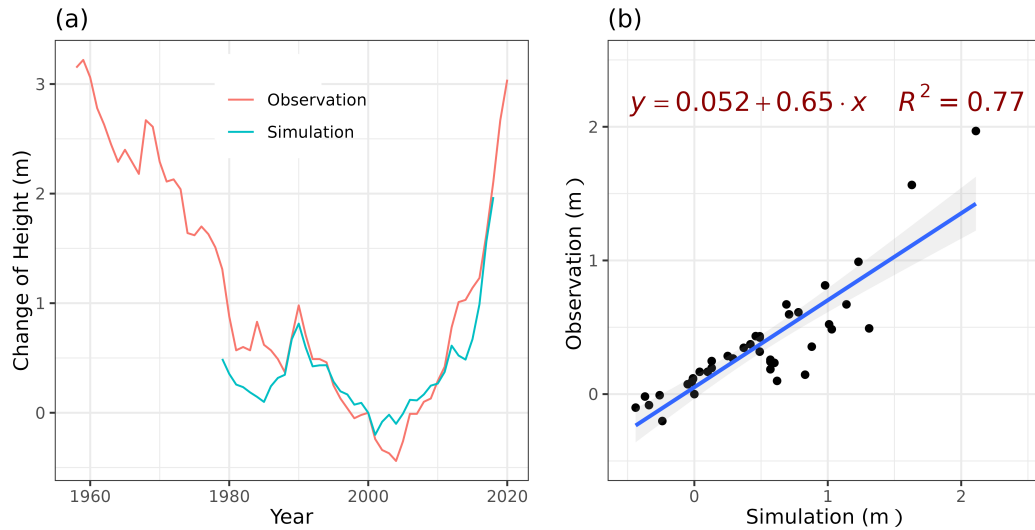
Figure 8. Changes in lake level, observation vs simulation, relative to the mean lake level in 2000 as the reference level. (a) Comparison of lake level changes; (b) Line-fit plot of simulated and observed values.

annually, while surface runoff (Q_s) and groundwater flow (Q_g) contribute a relatively minor ~~15 mm and 26 mm~~ 17 mm and 28 mm per year, respectively (Table 1).

~~Existing analyses, reliant on observational data, are limited to discerning contributions from the river, evaporation,~~

Table 1. Annual mean water balance components in Qinghai Lake from 1979 to 2018 as simulated by the coupled model.

Component	ΔS	P	E	R_i	Q_s	Q_g
Annual mean $(\times 10^8 \mathrm{m}^3)$	1.70	15.44	39.83	23.47	0.67	1.13
Annual mean (mm)	42	386	996	587	17	28
Percentage to P (%)	11.0	100	257.9	152.0	4.3	7.3

295

During the simulation period, with precipitation (P) as 100 units, evaporation (E) accounts for 258, river flux (R_i) in at 152, and surface (Q_s) and groundwater(Q_g) fluxes are 4 and ~~specified river outlets, and fail to distinguish the multitude of streams and surface and subsurface flows encircling the lake. Thus~~7 respectively. This sums up to a lake water mass increase (ΔS) of 11 units approximately. The contributions from surface and groundwater total 11 units, indicating that excluding

300 these contributions would result in non-increase in lake water. Though relatively small, the contributions from surface and groundwater are not negligible. Additionally, the mentioned surface and groundwater fluxes from SHUD model are only those entering the lake directly through its boundaries. Due to topographical factors, land surface and subsurface fluxes typically first enter rivers, then flow into the lake through these rivers. Areas directly contributing surface and subsurface fluxes to the lake without passing through rivers are very limited, usually confined to small sections along the lakeshore.

305 Due to differences in the algorithms used for water balance partitioning, our simulation results vary from those reported in other literature, with the literature indicating significantly higher groundwater contribution compared to our simulations (Li et al., 2007; Zhang et al., 2011; Cui and Li, 2016).

Table 2. Long-term average contributions of major rivers to Qinghai Lake and their respective percentages of total inflow, with comparable values from other literature.

Name	Area (km^2)	Modeling Q ($\times 10^8 \mathrm{m}^3$)	%	Li et al. (2007)(1959-2000) Min	Max	Average	%	Cui and Li (2015a, 2016)(1960-2010) Average	%
Buha R.	14932	10.96	46.7%	1.99	16.63	7.85	48.7%	8.09	45.5%
Quanji R.	599	0.72	3.1%	0.079	0.86	0.55	3.4%	0.54	3.0%
Shaliu R.	1645	1.68	7.1%	1.05	3.92	2.46	15.3%	3.12	17.5%
Haergai R.	1572	1.99	8.5%	1.96	3.35	2.42	15.0%	2.42	13.6%
Daotang R.	818	0.33	1.4%	-	-	-	-	-	-
Heima R.	123	0.26	1.1%	0.016	0.41	0.11	0.7%	0.11	0.6%
Major river	19689	15.94	67.9%	5.095	25.17	13.39	83.1%	14.28	80.3%
Land Area	25210	23.48	100%	-	-	16.12	100%	17.78	100%

Six major rivers flow into Qinghai Lake: the Buha, Shaliu, Quanji, Haergai, Daotang, and Heima rivers. Collectively, they contribute approximately $15.94 \times 10^8 m^3/a$, which represents 66.8% of the lake's total runoff of $23.48 \times 10^8 m^3/a$ (Table 2).
310 The catchment areas of these six rivers encompass 78% of the land area, contributing 67.9% of the total runoff to Qinghai Lake. Notably, the Buha River is the largest contributor, accounting for 46.7% of the total runoff into the lake.

Upon comparing our simulated results with historical literature (Li et al., 2007; Zhang et al., 2011; Cui and Li, 2015b, 2016; Zhang, 202 , we observe that while our findings are reliable, they exhibit discrepancies with previously reported data. The literature indicates a total river runoff recharge of approximately $17.78 \times 10^8 m^3/a$, with five rivers accounting for an annual runoff
315 of $14.28 \times 10^8 m^3/a$. Although the contributions from the major rivers are comparable, the total runoff recharge reported in the literature significantly differs from our findings, leading to notable variances in the contribution percentages. The total runoff data in these publications are based on a 1994 report (Lanzhou Branch of Chinese Academy of Sciences, 1994). In contrast, recent provincial water resources bulletins (Qinghai Provincial Department of Water Resources, 2022) suggest a multi-year average runoff in the Qinghai Lake basin ranging between 22.2-$26.7 \times 10^8 m^3/a$, aligning more closely with our simulation
320 results. These variances underscore the necessity for further research.

Despite discrepancies, our simulation underscores the need for further research and confirms the model's relevance for lake basin studies. While it's challenging to claim new findings for Qinghai Lake research from our limited data analysis, our model emerges as ~~an innovative tool for in-depth analysis of lake~~ a valuable tool for future research, offering a robust framework to enhance understanding of the lake's hydrology.
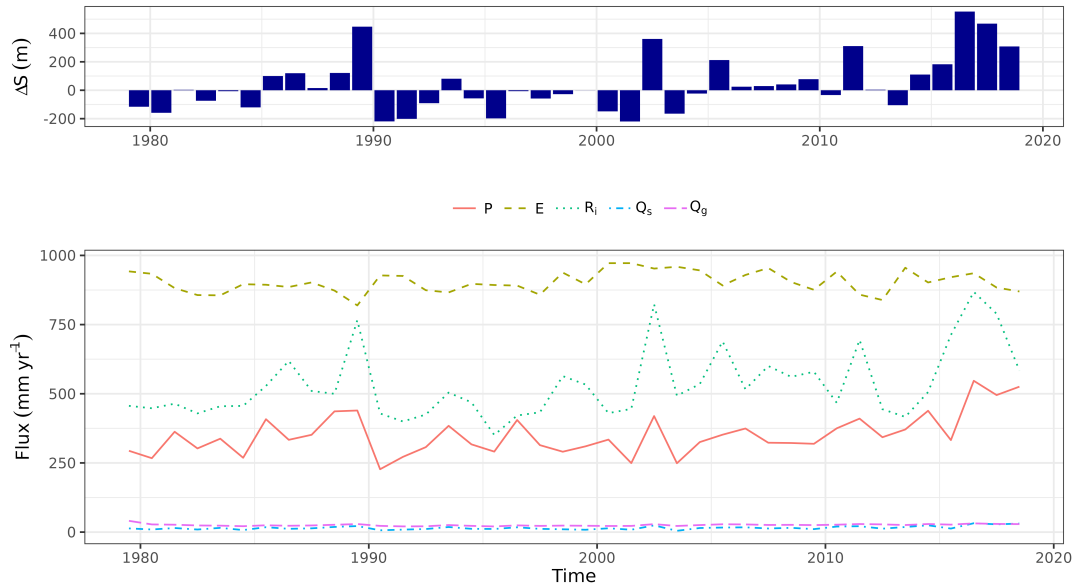
Figure 9. The water balance of Qinghai Lake, including six components: change in lake storage (ΔS), precipitation (P), evaporation (E), and contributions from rivers (R_i), surface runoff (Q_s), and groundwater flow (Q_g).

4 Discussion

It is noteworthy that the current lake coupling scheme is specifically designed for closed lakes, as the algorithm to handle downstream outlets has yet to be incorporated, though this limitation is not insurmountable and will be addressed in future updates. The model presently implies that the calculated top surface area of the lake does not influence the adjacent land elements. In essence, land elements remain static and do not transition into lake elements when the lake expands; the number of lake elements is maintained as constant. Higher levels of lake dynamics complexity are typically accommodated by employing 2D or 3D computational fluid dynamics (CFD) or hydrodynamics which offer a more granular understanding of lake behaviors and superior spatial resolution compared to hydrological models (Munar et al., 2018). As such, we underscore that the coupled model contributes invaluable data on rivers, surface, and subsurface flows at the basin scale, furnishing detailed boundary conditions integral for further studies in hydrodynamics, limnology, or biogeochemical cycles (Cobourn et al., 2018; Ladwig et al., 2021).

We acknowledge that the GOF measures for streamflow in the calibration and validation periods could be enhanced with additional model improvements. Upon scrutiny of the time-series of streamflow, we observed that the present hydrological model falls short in simulating the perennial and seasonal permafrost prevalent in this region. The high-altitude area of the QLB is characterized by perennial permafrost, while the regions surrounding the lake feature seasonal permafrost. The dynamism of permafrost exerts a substantial influence on hydrological processes, particularly on surface and subsurface flows. In the cold season, we noted that river discharge tends to approach zero, with distinct freeze-thaw phases, but the simulated streamflow

fails to accurately capture these dynamics. This shortcoming is attributable to the hydrological modeling rather than the lake-watershed coupling study. Nevertheless, it highlights the need to devise a novel algorithm for permafrost dynamics when deploying the model in cold regions. Additionally, the utilization of data more reliable than reanalysis data, which often underestimates heavy rainfall and rainfall intensity, could potentially improve the GOF measures.

We observe that the simulated lake level underestimates the measurements at the onset of the simulation period (1979-1987), a discrepancy likely stemming from low initial conditions for the lake level. Given the pronounced impact of the initial lake level on the ultimate outcome, it is imperative to exercise rigorous methodological consistency when setting the initial conditions of the lake in the modeling process.

5 Conclusion

In this study, we have introduced a novel methodology for coupling lake-watershed models and showcased its implementation in the Qinghai Lake Basin. Our model capably simulates lake level dynamics and offers an all-encompassing analysis of the lake's water balance. The model's ability to faithfully replicate observed changes in lake level and streamflow at the Buha River station underscores its potential value for hydrological studies in regions abundant with lakes.

The model provides fresh insights into lake hydrology, distinguishing the contributions of various components such as river inflow, surface runoff, and groundwater flow. This level of detail, unachievable solely through observational data, augments our understanding of hydrological processes occurring in lake basins. However, it should be noted that the current scheme is limited to closed lakes, and it does not take into account the dynamic expansion and contraction of lakes. These limitations are set to be addressed in future updates, further augmenting the model's versatility. The model's performance could be elevated further by incorporating more reliable data sources and refining the model's algorithms. A particular area for future enhancement is the simulation of permafrost dynamics, which significantly influence hydrological processes in cold regions.

As a hydrological model, SHUD primarily focuses on watershed hydrology and the horizontal water exchanges between the lake and its surrounding land. It employs a simplified potential evapotranspiration scheme to address the energy fluxes and atmosphere-land interactions often examined in land surface model (such as CLM and NOAH). Therefore, the proficiency of land surface models in vertical energy coupled with SHUD's expertise in horizontal hydrological processes hints at a potential for coupling. Such coupling could furnish a more refined depiction of water and energy storage and movement within lakes and watersheds.

In conclusion, the lake-watershed fully-coupled model developed in this study signifies a substantial advancement in the realm of hydrological modeling. While there are areas that necessitate further improvement and expansion, the model presents a potent tool for understanding and predicting hydrological processes in lake basins. Its successful deployment in the Qinghai Lake Basin illustrates its potential for wider application in hydrological studies and water resources management.

Code and data availability. All the source code and data in this paper, are saved in Zenodo (Shu, 2023a), except the observational streamflow in Buha River Gauge Station.

In addition to the Zenodo repository, we also store all source code on Github.

375 SHUD model: https://github.com/SHUD-System/SHUD (Shu et al., 2020).

rSHUD package: https://github.com/SHUD-System/rSHUD (Shu et al., 2023).

AutoSHUD: https://github.com/SHUD-System/AutoSHUD.

Author contributions. L. Shu and X. Li – Conceptualization, Investigation, Methodology, Software, Validation, Visualization, Writing original draft and editing. Y. Chang, X. Meng, H. Chen, S. Lyu – Supervision, Investigation, Writing original draft and editing. Z. Li, H. Wang,

380 Y. Qi.– Data preparation, Code development, program test, editing.

Competing interests. The authors declare that no competing interests are present.

Disclaimer. TEXT

Acknowledgements. This study is funded by the ~~Chinese Academy Sciences (E0290304,~~ National Natural Science Foundation of China (41930759), West Light Foundation of the Chinese Academy of Sciences (xbzg-zdsys-202215), ~~the Qinghai Key Laboratory of Disaster~~

385 ~~Prevention (QFZ-2021-Z02), the~~ National Natural Science Foundation of China (~~41930759,~~ 41961012), ~~West Light Foundation of~~ the Chinese Academy ~~of Sciences (2020-1-1)and~~ Sciences Talents Program, the Qinghai Key Laboratory of Disaster Prevention (QFZ-2021-Z02), National Cryosphere Desert Data Center (E01Z790215), Gansu Provincial Science and Technology Program (22ZD6FA005), and Lanzhou Science and Technology Plan Projects in 2023 (2023-1-49).

The GPT-4 (https://chat.openai.com) only assisted in language refinement.

References

Broxton, P. D., Zeng, X., Sulla-Menashe, D., and Troch, P. A.: A Global Land Cover Climatology Using MODIS Data, Journal of Applied Meteorology and Climatology, 53, 1593–1605, https://doi.org/10.1175/JAMC-D-13-0270.1, 2014.

Carter, V.: An overview of the hydrologic concerns related to wetlands in the United States., Canadian Journal of Botany, 64, 364–374, https://doi.org/10.1139/b86-053, 1986.

Chauvelon, P., Tournoud, M. G., and Sandoz, A.: Integrated hydrological modelling of a managed coastal Mediterranean wetland (Rhone delta, France): Initial calibration, Hydrology and Earth System Sciences, 7, 123–131, https://doi.org/10.5194/hess-7-123-2003, 2003.

Cobourn, K. M., Carey, C. C., Boyle, K. J., Duffy, C., Dugan, H. A., Farrell, K. J., Fitchett, L., Hanson, P. C., Hart, J. A., Henson, V. R., Hetherington, A. L., Kemanian, A. R., Rudstam, L. G., Shu, L., Soranno, P. A., Sorice, M. G., Stachelek, J., Ward, N. K., Weathers, K. C., Weng, W., and Zhang, Y.: From concept to practice to policy: modeling coupled natural and human systems in lake catchments, Ecosphere, 9, e02 209, https://doi.org/10.1002/ecs2.2209, 2018.

Crowe, A. S. and Schwartz, F. W.: Simulation of lake-watershed systems. I. Description and sensitivity analysis of the model, Journal of Hydrology, 52, 71–105, https://doi.org/10.1016/0022-1694(81)90097-4, 1981.

Cui, B. L. and Li, X. Y.: Runoff processes in the Qinghai Lake Basin, Northeast Qinghai-Tibet Plateau, China: Insights from stable isotope and hydrochemistry, Quaternary International, 380-381, 123–132, https://doi.org/10.1016/j.quaint.2015.02.030, 2015a.

Cui, B. L. and Li, X. Y.: Runoff processes in the Qinghai Lake Basin, Northeast Qinghai-Tibet Plateau, China: Insights from stable isotope and hydrochemistry, Quaternary International, 380-381, 123–132, https://doi.org/10.1016/j.quaint.2015.02.030, 2015b.

Cui, B. L. and Li, X. Y.: The impact of climate changes on water level of Qinghai Lake in China over the past 50 years, Hydrology Research, 47, 532–542, https://doi.org/10.2166/nh.2015.237, 2016.

Dargahi, B. and Setegn, S. G.: Combined 3D hydrodynamic and watershed modelling of Lake Tana, Ethiopia, Journal of Hydrology, 398, 44–64, https://doi.org/10.1016/j.jhydrol.2010.12.009, 2011.

Dong, H., Song, Y., and Zhang, M.: Hydrological trend of qinghai lake over the last 60 years: Driven by climate variations or human activities?, Journal of Water and Climate Change, 10, 524–534, https://doi.org/10.2166/wcc.2018.033, 2019.

Freeze, R. and Harlan, R.: Blueprint for a physically-based, digitally-simulated hydrologic response model, Journal of Hydrology, 9, 237–258, https://doi.org/10.1016/0022-1694(69)90020-1, 1969.

Grant, L., Vanderkelen, I., Gudmundsson, L., Tan, Z., Perroud, M., Stepanenko, V. M., Debolskiy, A. V., Droppers, B., Janssen, A. B. G., Woolway, R. I., Choulga, M., Balsamo, G., Kirillin, G., Schewe, J., Zhao, F., del Valle, I. V., Golub, M., Pierson, D., Marcé, R., Seneviratne, S. I., and Thiery, W.: Attribution of global lake systems change to anthropogenic forcing, Nature Geoscience, 14, 849–854, https://doi.org/10.1038/s41561-021-00833-x, 2021.

Gupta, H. V., Kling, H., Yilmaz, K. K., and Martinez, G. F.: Decomposition of the mean squared error and NSE performance criteria: Implications for improving hydrological modelling, Journal of Hydrology, 377, 80–91, https://doi.org/10.1016/j.jhydrol.2009.08.003, 2009.

Hansen, N.: The CMA Evolution Strategy: A Comparing Review, in: Towards a New Evolutionary Computation, pp. 75–102, Springer-Verlag, Berlin/Heidelberg, https://doi.org/10.1007/11007937_4, 2016.

He, J., Yang, K., Tang, W., Lu, H., Qin, J., Chen, Y., and Li, X.: The first high-resolution meteorological forcing dataset for land process studies over China, Scientific Data, 7, 25, https://doi.org/10.1038/s41597-020-0369-y, 2020.

Hrachowitz, M. and Clark, M. P.: HESS Opinions: The complementary merits of competing modelling philosophies in hydrology, Hydrology and Earth System Sciences, 21, 3953–3973, https://doi.org/10.5194/hess-21-3953-2017, 2017.

Inoue, M., Park, D., Justic, D., and Wiseman, W. J.: A high-resolution integrated hydrology-hydrodynamic model of the Barataria Basin system, Environmental Modelling and Software, 23, 1122–1132, https://doi.org/10.1016/j.envsoft.2008.02.011, 2008.

Johnston, C. A. and Shmagin, B. A.: Scale Issues in Lake-Watershed Interactions: Assessing Shoreline Development Impacts on Water
430   Clarity, pp. 297–313, Springer Netherlands, Dordrecht, https://doi.org/10.1007/1-4020-4663-4_16, 2006.

Jones, B. M., Grosse, G., Farquharson, L. M., Roy-Léveillée, P., Veremeeva, A., Kanevskiy, M. Z., Gaglioti, B. V., Breen, A. L., Parsekian, A. D., Ulrich, M., and Hinkel, K. M.: Lake and drained lake basin systems in lowland permafrost regions, Nature Reviews Earth & Environment, 3, 85–98, https://doi.org/10.1038/s43017-021-00238-9, 2022.

Kratz, T. K., Webster, K. E., Bowser, C. J., Magnuson, J. J., and Benson, B. J.: The influence of landscape position on lakes in northern
435   Wisconsin, Freshwater Biology, 37, 209–217, https://doi.org/10.1046/j.1365-2427.1997.00149.x, 1997.

Ladwig, R., Hanson, P. C., Dugan, H. A., Carey, C. C., Zhang, Y., Shu, L., Duffy, C. J., and Cobourn, K. M.: Lake thermal structure drives interannual variability in summer anoxia dynamics in a eutrophic lake over 37 years, Hydrology and Earth System Sciences, 25, 1009–1032, https://doi.org/10.5194/hess-25-1009-2021, 2021.

Lanzhou Branch of Chinese Academy of Sciences: Environmental evolution and prediction in Qinghai Lake (in Chinese), Science Press,
440   Beijing, 1994.

Lewis, W. M., Saunders, J. F., Crumpacker, D. W., and Brendecke, C. M.: Total Nutrient Loading of the Lake, in: Eutrophication and Land Use: Lake Dillon, Colorado, pp. 131–139, Springer New York, New York, NY, https://doi.org/10.1007/978-1-4613-8277-5_13, 1984.

Li, X., Peng, S., Xi, Y., Woolway, R. I., and Liu, G.: Earlier ice loss accelerates lake warming in the Northern Hemisphere, Nature Communications, 13, https://doi.org/10.1038/s41467-022-32830-y, 2022.

445   Li, X. Y., Xu, H. Y., Sun, Y. L., Zhang, D. S., and Yang, Z. P.: Lake-level change and water balance analysis at lake Qinghai, West China during recent decades, Water Resources Management, 21, 1505–1516, https://doi.org/10.1007/s11269-006-9096-1, 2007.

Munar, A. M., Cavalcanti, J. R., Bravo, J. M., Fan, F. M., da Motta-Marques, D., and Fragoso, C. R.: Coupling large-scale hydrological and hydrodynamic modeling: Toward a better comprehension of watershed-shallow lake processes, Journal of Hydrology, 564, 424–441, https://doi.org/https://doi.org/10.1016/j.jhydrol.2018.07.045, 2018.

450   Nachtergaele, F., van Velthuizen, H., Verelst, L., Batjes, N., Dijkshoorn, J., van Engelen, V., Fischer, G., Jones, A., Montanarella, L., Petri, M., Prieler, S., Teixeira, E., Wilberg, D., and Shi, X.: Harmonized World Soil Database (version 1.2), Food and Agric Organization of the UN (FAO); International Inst. for Applied Systems Analysis (IIASA); ISRIC - World Soil Information; Inst of Soil Science-Chinese Acad of Sciences (ISS-CAS); EC-Joint Research Centre (JRC), 2008.

NASA, METI, AIST, Japan Spacesystems, and U.S./Japan ASTER Science Team: ASTER Global Digital Elevation Model V003,
455   https://doi.org/10.5067/ASTER/ASTGTM.003, 2018.

Nash, J. E. and Sutcliffe, J. V.: River Flow Forecasting Through Conceptual Models Part I-a Discussion of Principles*, Journal of Hydrology, 10, 282–290, https://doi.org/10.1016/0022-1694(70)90255-6, 1970.

Pi, X., Luo, Q., Feng, L., Xu, Y., Tang, J., Liang, X., Ma, E., Cheng, R., Fensholt, R., Brandt, M., Cai, X., Gibson, L., Liu, J., Zheng, C., Li, W., and Bryan, B. A.: Mapping global lake dynamics reveals the emerging roles of small lakes, Nature Communications, 13, 1–12,
460   https://doi.org/10.1038/s41467-022-33239-3, 2022.

Possa, T. M., Collares, G. L., dos Santos Boeira, L., Jardim, P. F., Fan, F. M., and Terra, V. S. S.: Fully coupled hydrological-hydrodynamic modeling of a basin-river-lake transboundary system in Southern South America, Journal of Hydroinformatics, 24, 93–112, https://doi.org/10.2166/HYDRO.2021.096, 2022.

Qi, Y., Lian, X., Wang, H., Zhang, J., and Yang, R.: Dynamic mechanism between human activities and ecosystem services: A case study of Qinghai lake watershed, China, Ecological Indicators, 117, https://doi.org/10.1016/j.ecolind.2020.106528, 2020.

Qinghai Provincial Department of Water Resources: 2021 Qinghai Province Water Resources Bulletin (in Chinese), Tech. rep., 2022.

Qu, Y. and Duffy, C. J.: A semidiscrete finite volume formulation for multiprocess watershed simulation, Water Resources Research, 43, 1–18, https://doi.org/10.1029/2006WR005752, 2007.

Shu, L.: Lake-Watershed coupling model in Qinghai Lake Basin, with SHUD model, https://doi.org/10.5281/zenodo.8106880, 2023a.

Shu, L.: SHUD-System/rSHUD: 2.0, https://doi.org/10.5281/zenodo.8104336, 2023b.

Shu, L., Ullrich, P. A., and Duffy, C. J.: Simulator for Hydrologic Unstructured Domains (SHUD v1.0): numerical modeling of watershed hydrology with the finite volume method, Geoscientific Model Development, 13, 2743–2762, https://doi.org/10.5194/gmd-13-2743-2020, 2020.

Shu, L., Ullrich, P., Meng, X., Duffy, C., Chen, H., and Li, Z.: rSHUD v2.0: Advancing Unstructured Hydrological Modeling in the R Environment, Geoscientific Model Development Discussions, 2023, 1–40, https://doi.org/10.5194/gmd-2023-128, 2023.

Su, D., Hu, X., Wen, L., Lyu, S., Gao, X., Zhao, L., Li, Z., Du, J., and Kirillin, G.: Numerical study on the response of the largest lake in China to climate change, Hydrology and Earth System Sciences, 23, 2093–2109, https://doi.org/10.5194/hess-23-2093-2019, 2019.

Su, D., Wen, L., Gao, X., Leppäranta, M., Song, X., Shi, Q., and Kirillin, G.: Effects of the Largest Lake of the Tibetan Plateau on the Regional Climate, Journal of Geophysical Research: Atmospheres, 125, 1–18, https://doi.org/10.1029/2020JD033396, 2020.

Wang, H., Qi, Y., Lian, X., Zhang, J., Yang, R., and Zhang, M.: Effects of climate change and land use/cover change on the volume of the Qinghai Lake in China, Journal of Arid Land, 14, 245–261, https://doi.org/10.1007/s40333-022-0062-4, 2022.

Woolway, R. I.: The pace of shifting seasons in lakes, Nature communications, 14, 2101, https://doi.org/10.1038/s41467-023-37810-4, 2023.

Woolway, R. I., Jennings, E., Shatwell, T., Golub, M., Pierson, D. C., and Maberly, S. C.: Lake heatwaves under climate change, Nature, 589, 402–407, https://doi.org/10.1038/s41586-020-03119-1, 2021.

Wu, B., Wang, G., Wang, Z., Liu, C., and Ma, J.: Integrated hydrologic and hydrodynamic modeling to assess water exchange in a data-scarce reservoir, Journal of Hydrology, 555, 15–30, https://doi.org/10.1016/j.jhydrol.2017.09.057, 2017.

Xu, Z., Godrej, A. N., and Grizzard, T. J.: The hydrological calibration and validation of a complexly-linked watershed-reservoir model for the Occoquan watershed, Virginia, Journal of Hydrology, 345, 167–183, https://doi.org/10.1016/j.jhydrol.2007.07.015, 2007.

Ye, X., Zhang, Q., Bai, L., and Hu, Q.: A modeling study of catchment discharge to Poyang Lake under future climate in China, Quaternary International, 244, 221–229, https://doi.org/10.1016/j.quaint.2010.07.004, 2011.

Zhang, G.: Qinghai Lake hydrology and climate data (1956-2020), https://doi.org/10.1080/27669645.2021.2015870, 2021.

Zhang, G., Xie, H., Duan, S., Tian, M., and Yi, D.: Water level variation of Lake Qinghai from satellite and in situ measurements under climate change, Journal of Applied Remote Sensing, 5, 053 532, https://doi.org/10.1117/1.3601363, 2011.

Zhang, G., Xie, H., Yao, T., Li, H., and Duan, S.: Quantitative water resources assessment of Qinghai Lake basin using Snowmelt Runoff Model (SRM), Journal of Hydrology, 519, 976–987, https://doi.org/10.1016/j.jhydrol.2014.08.022, 2014.

Zhang, Q. and Werner, A. D.: Integrated surface-subsurface modeling of Fuxianhu Lake catchment, Southwest China, Water Resources Management, 23, 2189–2204, https://doi.org/10.1007/s11269-008-9377-y, 2009.